# Thermodynamics and kinetics of CO and benzene adsorption on Pt(111) studied with pulsed molecular beams and microcalorimetry

Alexander Schießer[1,*], Peter Hörtz, Rolf Schäfer

*Eduard-Zintl-Institut für Anorganische und Physikalische Chemie, Technische Universität Darmstadt, Petersenstraße 20, 64287 Darmstadt, Germany*

**Abstract**

The adsorption and desorption of CO and benzene on Pt(111) has been investigated with pulsed molecular beams in combination with a microcalorimeter. For benzene the sticking probability has been measured in dependence of coverage $\theta$ at 300K. For coverages $\theta > 0.8$ partially transient adsorption is observed. From an analysis of the time-dependence of the molecular beam pulses the rate constant for desorption is determined to 5.6/s. With a precursor-mediated kinetic adsorption model this allows one to obtain also the hopping rate constant of 95.5/s. The measured adsorption enthalpies could be best described by $200 - 96\theta - 33\theta^2$kJ/mol in very good agreement with literature values. For CO on Pt(111) also transient adsorption has been observed for $\theta > 0.95$ at 300K. The kinetic analysis yields rate constants for desorption and hopping of 20/s and 51/s, respectively. The heats of adsorption show a linear dependence on coverage ??−??$\theta$kJ/mol between $0 \leq \theta \leq 0.8$, which is in good agreement with recent thermodesorption data and quantum chemical calculations.

*Keywords:*

## 1. Introduction

The modification of surfaces and interfaces and the control of their physico-chemical properties is of fundamental interest for various disciplines. For example, the adsorption of gaseous compounds as the first step in a heterogeneously, catalyzed chemical reaction determines decisively the performance of the catalyst. Therefore, the experimentally determined heat of adsorption is very useful for a comparison of different catalysts and a key property to discuss the microscopic processes involved in heterogenous catalysis. In order to measure the adsorption enthalpy, different methods have been developed. Often temperature-programmed techniques has been used, giving rise to a desorption of the adsorbate, which itself is followed by mass spectrometry. A kinetic modeling of the desorption progress then allows one to extract the activation energy of the desorption process. For the case of a vanishing energy barrier this gives one then also the heat of adsorption. In order to avoid the determination of adsorption heats from kinetic data, a direct method for the measurement of adsorption enthalpies is necessary. Early attempts of determining adsorption heats on single crystals directly with calorimetry were made by Kyser and Masel and Kovar et al.. But the first single crystal adsorption calorimeter (SCAC) giving data for various systems was pioneered by King and coworkers. In their setup a pulsed molecular beam was used in combination with a mercury-cadmium-telluride (MCT) detector to measure adsorption enthalpies of gaseous compounds on various single crystal surfaces. Campbell and coworkers improved the sensitivity of the SCAC by using a pyroelectric polyvinylidene fluoride (PVDF) foil in mechanical contact with a thin substrate to study adsorption of low vapor pressure molecules[27,26]. We have also developed an adsorption microcalorimeter combined with a pulsed molecular beam source, which allows one to study the adsorption thermodynamics and desorption kinetics of high as well

*Corresponding author
*Email address:*
schiesser@cluster.pc.chemie.tu-darmstadt.de
(Alexander Schießer)

as low vapor pressure molecules. Within this article results are presented for CO and benzene on Pt(111). The Pt(111) surface has been chosen because recent calorimetric data are already available for benzene adsorption, which allows us to validate the functioning of our setup. For the adsorption of CO on Pt(111) only an older set of calorimetric data exists, which shows some discrepancies to thermodesorption experiments and recent quantum chemical calculations. Therefore, we have reinvestigated the adsorption enthaplies for CO on Pt(111) with an independent setup in order to contribute new calorimetric results.

## 2. Experimental

The experiments were performed in two stainless steel ultrahigh vacuum (UHV) chambers, separated by a gate valve and with base pressures ¡ $5 \cdot 10^{-10}$ mbar. The sample preparation chamber was equipped with a turbo molecular pump (pumping speed 170 L/s) and contains an Argon sputter gun, a radiative heater (250W-filament) and a low energy electron diffraction optics (MiniLEED from OCI). The SCAC chamber with a volume of about 15 L is pumped by a turbo molecular pump (pumping speed 450 L/s) and holds the calorimeter, a pulsed molecular beam source and a quadrupole mass spectrometer (QMS 112 from Balzers), that is placed neither in the line of sight of the source nor of the sample.

### *2.0.1. Sample Preparation*

A 2µm thick Pt(111) single crystal (Mateck) was sandwiched between two 100µm Ta sheets (12x12mm), each had a 7mm diam hole in the center. After spot welding them, the obtained sandwich was mounted on a sample holder, containing a 8mm diam hole, in order to provide access to the back side of the sample. Then the sample was cleaned by Ar sputtering (750V, 5µA/cm$^2$) and annealing in $5 \cdot 10^{-7}$mbar $O_2$ at 850K by radiative heating with the tungsten filament located 4mm from the back side of the Pt(111). Sputtering and annealing cycles followed by flash annealing to 1000K were repeated until the single crystal revealed good LEED patterns (Referenz: LEED-Bild in elektronisches Zusatzmaterial). After cooling to room temperature, the cleaned sample was transferred from the preparation chamber into the SCAC chamber.

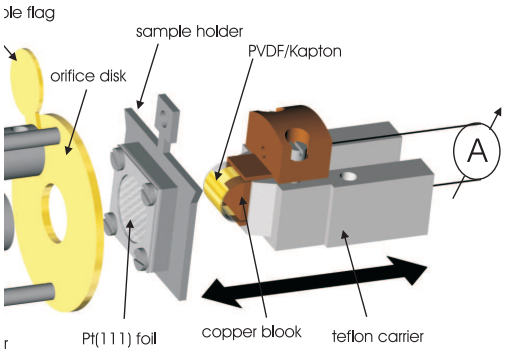


Figure 1: Schematic setup of the SCAC setup: To start a calorimetric measurement the teflon carrier is moved towards the sample holder until mechanical contact is reached and then both are driven together close to the orifice disk

### *2.0.2. Molecular Beam Source*

The main difference compared to Campbells SCAC setup is the piezoelectric pulsed molecular beam source[23], which allows one to investigate both low and high vapor pressure molecules. A piezoelectric disk translator, driven by a high voltage pulse, opens a nozzle which allows the molecules of the vapor phase to escape from the gas reservoir, thereby forming a pulsed molecular beam, which enters the sample in the SCAC chamber. From the pressure decrease in the gas reservoir after several pulses one can easily calculate the number of molecules per pulse by applying the ideal gas law. In the present experiments the reservoir contains about 1 mbar of either anhydrous benzene (99.8% purity) or CO (99.97% purity). The beam source was operated with pulses of 50ms duration and a repetition rate of 0.5 Hz. This results in a temporary pressure increase of typically $3 \cdot 10^{-8}$ mbar.

### *2.0.3. Measurement of heats of adsorption*

In Figure 1 a schematic setup of the SCAC is presented.

The calorimeter design follows that of Campbells group **(Lit.)**. To be more specific, it consists of a 9µm thick pyroelectric polymer ribbon ($\beta$-polyvinylidene difluoride, PVDF) (6mm x 25mm) with gold electrodes on both sides for electric contact. This ribbon is clamped (together with a 25µm Kapton foil to provide a better mechanical stiffness) between copper blocks to built an arc. The PVDF/Kapton arc is gently pressed to the

back side of the cleaned Pt(111) to guarantee thermal contact.
The pulsed molecular beam source is placed in front of the sample. At a distance of 6mm from the source a gold plated orifice disk and a gold flag, which covers the orifice (7mm diam hole), are mounted. Together with the calorimeter, the sample was driven in front of the orifice (flag closed), and the pulsed molecular beam source was switched on.
All molecules coming from the source were scattered by the flag or the orifice disk, and thus could not reach the Pt(111). After a few pulses the flag was opened and the molecules could impinge onto the Pt(111) surface. The orifice disk provided that only molecules heading for the Pt(111) were able to pass - undesired adsorption on other parts was avoided. The adsorption of molecules caused an increase of the temperature of the Pt(111) surface and also of the pyroelectric PVDF foil. The pyroelectric current was amplified with a current-to-voltage converter by a factor of $10^{11}$V/A. During each SCAC experiment the pyroelectric signal, the signal from the pressure decrease in the reservoir of the pulsed molecular beam source as well as the signal of the quadrupole mass spectrometer (QMS) were collected synchronously via USB6008 (from National Instruments). After the adsorption process was finished, the gold flag was closed again to proof the stability of the molecule beam source.

Before and after such a calorimetric measurement, calibration of the micro-calorimeter was carried out with laser pulses striking the front side of the single crystal surface through a view port. Generation of the laser pulses (50ms length) of known energy was achieved with a diode laser (645nm), a tailor made laser shutter[19] and a NIST certified photo diode. Furthermore for the calibration the reflectivity of the Pt(111) foil of 0.74 at 645 nm and losses due to absorption of the view port had to be taken into account. The pyroelectric peak current was proofed being proportional to the absorbed laser energy between 0 - 50μJ.
Measuring the pyroelectric current directly with a current-to-voltage converter has the advantage that the electric capacity of the detector does not influence the signal. Thus we do not need to reconstruct the shape of the pyroelectric signal when desorption occurs, in contrast to the procedure applied by Campbell and coworkers[10]. The pulse-to-pulse standard deviation of the measured heats of adsorption is about 10-15nJ, similar to the accuracy reported in literature, although our single crystal was twice as thick[18].

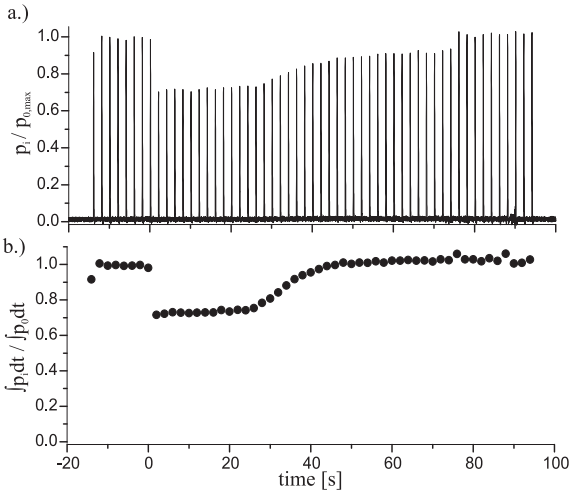


Figure 2: (a) Normalized QMS signal (78amu) for the adsorption of benzene on Pt(111) at 300K. After eight pulses (each containing $1.8 \cdot 10^{13}$ benzene molecules) the flag was opened, after 37 pulses the flag was closed again. (b) The circles refer to the normalized area under the QMS signal for each pulse.

## 3. Results and discussion

### *3.1. Benzene*

#### *3.1.1. Net sticking probability*

Typical QMS data collected during a SCAC experiment for benzene on Pt(111) are shown in Figure 2(a). After the gold flag was opened, the QMS peaks were diminished due to the adsorption of benzene. Following a period of constant adsorption, the QMS peaks increased and start to saturate. According to the method originally developed by King and Wells[11] the *net sticking probability* is calculated from the total area under the QMS signal for each pulse $\int p_i dt$

$$s_{i,net} = \frac{1}{f}\left(1 - \frac{\int p_i dt}{\int p_0 dt}\right), \qquad (1)$$

wherein $\int p_0 dt$ corresponds to the area under the peak of the QMS signal for pulses with the flag closed. The normalized areas under the QMS signal are shown in shown in 2(b). From this it becomes

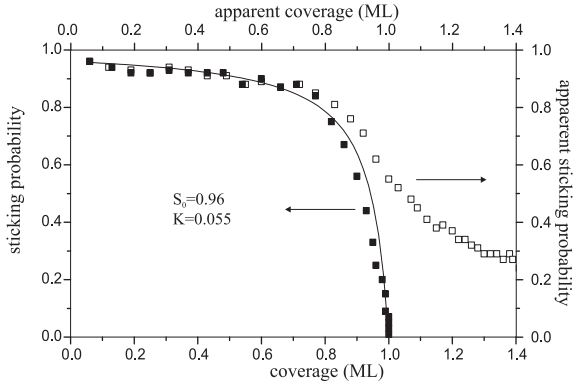


Figure 3: Coverage dependence of the apparent and net sticking probability for benzene on clean Pt(111) at T=300K. A model for precursor-mediated adsorption is fit to the data using the Kisliuk equation (4) (solidcurve). One monolayer (ML) corresponds to $2.3 \cdot 10^{14}$ molecules/cm$^2$

clear that the net adsorption terminates about 25 - 30 pulses after opening the flag. The fraction of impinging molecules intercepted by the crystal surface $f$ was determined to be $0.31 \pm 0.01$, assuming that the initial sticking probability of benzene is $0.96 \pm 0.01$ as reported in literature[2].

Defining a monolayer as the saturation coverage at 300K, a monolayer is reached as soon as the net sticking probability attains zero. Considering the number of molecules per pulse (determined from the pressure decrease in the reservoir of the pulsed molecular beam source) permits one to obtain $N^{ads}_{i,net}$, i. e. the net number of adsorbed molecules per pulse

$$N^{ads}_{i,net} = N_{pulse} \cdot f \cdot s_{i,net}. \tag{2}$$

Summation over all pulses reveals for a monolayer $8.4 \cdot 10^{13}$ molecules adsorbed on the Pt(111) surface with an area of 0.38cm$^2$at 300K. This is in good accordance with the literature value of a monolayer $2.3 \cdot 10^{14}$/cm$^2$ [10]. Thus the total coverage after each pulse $i$ is given by

$$\theta_i = \frac{\sum_{i=1}^{i} N^{ads}_{i,net}}{\sum_{i=1}^{i=\infty} N^{ads}_{i,net}} = \frac{\sum_{i=1}^{i} s_{i,net}}{\sum_{i=1}^{i=\infty} s_{i,net}}. \tag{3}$$

The coverage dependence of the net sticking probability is displayed in Figure 3.

The coverage dependence of the sticking probability on flat metal surfaces is often described by a precursor-mediated behavior. This model was introduced by Kisliuk[13], where the sticking probability is expressed in dependence of the coverage $\theta$ and the initial sticking probability $s_o$

$$s = \frac{s_o}{1 + K(\frac{\theta}{1-\theta})}. \tag{4}$$

The parameter K describes the degree of mobility of the precursor state: small positive values of K correspond to a highly mobile precursor, while $K \to 1$ describes an immobile precursor and hence a simple Langmuir kinetics. The Kisliuk model neglects adsorbate interactions other than site blocking and ad-layer ordering.
Using eq.4 to fit the coverage dependence of the net sticking probability, as shown in 3, an initial sticking probality of $s_o = 0.96 \pm 0.01$ and a Kisliuk parameter of $K = 0.055 \pm 0.010$ is found, which in good agreement with the value of (0.035) reported by Campbell and coworkers[10].

*3.1.2. Desorption kinetics at $\theta \approx 1$*

With pulsed experiments desorption between the pulses could be observed from a comparison of the peak maxima with respect to the area under the QMS signals. Whilst the area under the QMS signal for each pulse includes the non sticking molecules plus the molecules eventually desorbed between the pulses, the height $p_{i,max}$ of the QMS signals only contains the molecules that never stuck on the single crystal surface. In order to take also the transiently adsorbed molecules into account, a so-called *apparent sticking probability* is introduced, which is given in analogy to eq.1 for each pulse by

$$s_{i,app} = \frac{1}{f}\left(1 - \frac{p_{i,max}}{p_{0,max}}\right), \tag{5}$$

but now the peak heights have to be used for the calculation of $s_{i,app}$. With the number of apparently adsorbed molecules per pulse $N^{ads}_{i,app}$ the apparent coverage could be determined in the same way as the net coverage was calculated. Since the apparent sticking probability takes also the transiently adsorbed molecules into account, the apparent coverage just appears to be greater than unity. This is, because desorption between the pulses is not considered. Also the apparent sticking probability is displayed as a function of their coverage in Figure 3. It is obvious that the net and the apparent sticking probability shows

the same behavior for a coverage ranging from $\theta = 0 - 0.8$, but then the net sticking probability tends to zero, while the apparent stick probability remains finite and tends towards a constant value, i. e. at $\theta > 0.8$ a part of the benzene molecules are transiently adsorbed and become desorbed in the period of 2s between the gas pulses.

In order to learn more about this desorption process, a simple kinetic model of consecutive elementary steps is used. Let us consider that a molecular gas pulse was applied, and that the number of intermediately, transiently adsorbed molecules $A_{ads}$ is given by $N_{A_{ads}(0)}$. These molecules leave the surface with a desorption rate constant $k_d = 1/\tau_d$, i.e. the transiently adsorbed molecules can be found in the gas phase after they persisted on the surface with a residence time of $\tau_d$. The desorbed molecules $A_g$ stay for a certain time in the gas phase $\tau_p$ before they exit the vacuum chamber through the turbo molecular pump, which is determined by the pumping rate constant $k_p = 1/\tau_p$.

The kinetic model with the consecutive reaction steps is therefore described by

$$A_{ads} \overset{k_d}{\rightarrow} A_g \overset{k_p}{\rightarrow} A_{pump} \qquad (6)$$

Furthermore, one has to take into account, that there are still molecules in the gas phase which never stuck to the surface. The number of these molecules amounts to $N_{A_g(0)}$. Hence the total number of molecules in the gas phase $N_{A_g}$, which is measured directly with the QMS, is given by

$$N_{A_g}(t) = (N_{A_g(0)} + \tfrac{k_d}{k_p - k_d} N_{A_{ads}(0)}) \cdot e^{-t/\tau_p} + \tfrac{k_d}{k_p - k_d} N_{A_{ads}(0)} \cdot e^{-t/\tau_d}. \qquad (7)$$

If the flag is closed, neither permanent nor transient adsorption takes place, thus eq.7 will reduce to

$$N'_{A_g}(t) = N'_{A_g(0)} \cdot e^{-t/\tau_p}. \qquad (8)$$

Fitting this function to the tail of a QMS signal with the gold flag closed yields $\tau_p = 36$ms, or $k_p = 28s^{-1}$ respectively. This pumping rate constant is close to the value estimated from the pumping speed and the volume of the UHV chamber ($450\text{L/s}/15\text{L} = 30s^{-1}$).

In Figure 4 two QMS signals are displayed, a QMS peak, resulting from s molecular gas pulse with closed flag (dashed line), and another QMS peak at a coverage of $\theta \approx 1$ (solid line). Obviously

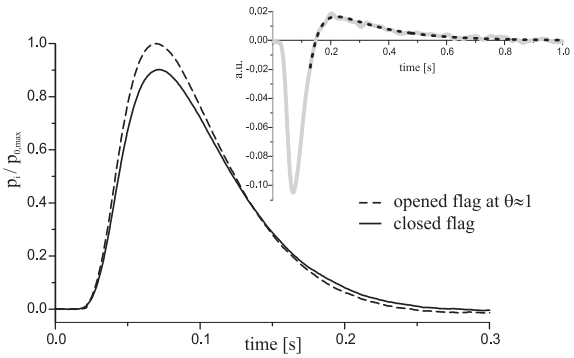


Figure 4: Transient adsorption behavior at $\theta \approx 1$. Averaged QMS peaks with closed flag (dashed line) and open flag at $\theta \approx 1$ (solid line). The difference (gray line) between these two QMS peaks is shown in the inset. The doted line is the fit taking eq.7 and eq.8 into account.

the peak with the closed flag is higher in magnitude but declines faster than the one with the open flag, because no transient adsorption followed by desorption takes place. However, the area (from 0 to 2s) under both peaks are equal as can be seen from Fig.2. In order to illustrate the different behavior of the two QMS signals the difference between them is shown in the inset of Figure 4. The desorption rate constant is obtained by adjusting $N_{A_g}(t) - N'_{A_g}(t)$ with the help of eq.7 and eq.8 to the measured data (dashed line in Fig.4), revealing a residence time at $\theta \approx 1$ of $\tau_d = 180 \pm 20$ms, i.e. $k_d = 5.6\text{s}^{-1}$. The Gibbs energy of activation for the desorption process $\Delta\ddagger G = ln(k_d/\upsilon)RT$ may be estimated from the obtained $k_d$ and a pre-exponential factor using transition state theory of $\upsilon = \mathbf{kT/h}{=}6.25 \cdot 10^{12} s^{-1}$, yielding a value of 67kJ/mol. This value is in good agreement with Ihm et al., but we could not identify two different binding sites like they postulated.

*3.1.3. Microcalorimetry*

Typical pyroelectric data collected during a SCAC experiment for benzene on Pt(111) are shown in Figure 5. The peak heights of the pyroelectric current are proportional to the heat released during adsorption. The peak heights are decreasing nearly in a linear fashion for the first 13 benzene pulses, even if a constant sticking probability was observed. Then the pyroelectric signals first decrease faster before they reach a constant value. The differential molar heats of adsorption $q_{cal}$ are calculated by dividing the heat released during the adsorption process through the appar-

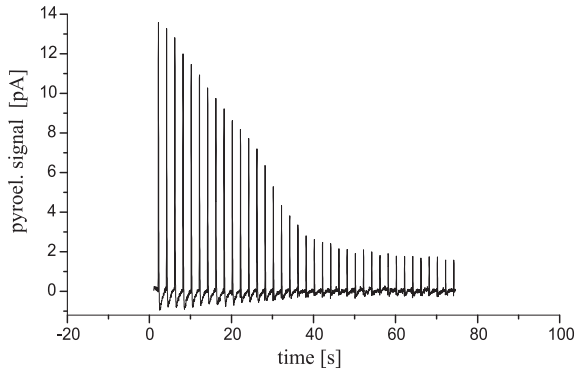


Figure 5: Pyroelectric signals for the adsorption of benzene on Pt(111), recorded to together with the QMS data, depicted in Figure 2

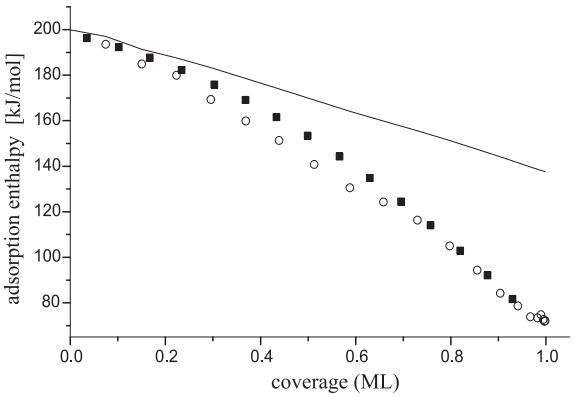


Figure 6: Average of four measurements (open circles) of the differential molar adsorption enthalpies compared with the data of Campbell (filled squares); solid line: integrated molar adsorption enthalpies.

ent mole number of adsorbed molecules $n_{i,app}^{ads}$. The apparent number of adsorbed moles is used, because the height of the detected heat signals is only due to benzene adsorption. The desorption process could not be detected calorimetrically because the heat during desorption is consumed over a large time interval of about a few hundred milliseconds and could therefore not be extracted out of the noise of the calorimeter signal. However, the observed heats for each pulse $q_{cal,i}$ have to be assigned to the coverage $\theta_i$ arising from the net sticking probability. In a last step, the increased kinetic energy of the benzene molecules in the thermal molecular beam has to be considered. Thus the observed heats $q_{cal}$ have to be corrected

$$q_{ads} = \Delta H_{ads} = -(q_{cal} + \frac{1}{2}RT), \qquad (9)$$

in order to obtain the differential molar adsorption enthalpies $\Delta H_{ads}$, which are shown in Figure 6.

The thin solid line in the Figure 6 belongs to the integral heats of adsorption

$$\Delta H_{ads,integ} = \frac{\sum_0^i \Delta H_{ads}(\theta_i)}{\sum_0^1 \theta_i}. \qquad (10)$$

The measured coverage dependent differential heat of adsorption decrease from 200kJ/mol ($\theta = 0$) to 72 kJ/mol ($\theta \approx 1$). The coverage dependence could be described best by $200 - 96\theta - 33\theta^2$kJ/mol. The data are in nearly perfect agreement with the ones published by Ihm et al., despite the slightly lower values for a coverage ranging between $\theta = 0.3$ to $\theta = 0.6$. The relative error is estimated to be 5 kJ/mol, and the absolute error is about 5%, mainly caused by uncertainties in determining the optical reflectivity of the sample.

### *3.2. CO*

#### *3.2.1. Net sticking probability*

Typical data collected during a SCAC experiment for CO on Pt(111) are shown in Figure 7. After opening the flag, the QMS peaks are steadily recovering, but do not reach the original peak height with the flag closed again.

In analogy to benzene, the net sticking probability was calculated with eq.1 using the same fraction of $f = 0.31$. The coverage was determined with eq.3 yielding a saturation coverage of $7.5 \cdot 10^{14}$molecules/cm$^2$, a value that is in the best congruence with the literature. In our definition this equals a monolayer. However, often in the literature a monolayer is defined as one adsorbate molecule per substrate atom. Within this definition a monolayer corresponds to $1.505 \cdot 10^{15}$molecules/cm$^2$ [7], which is almost exactly twice the number of adsorbed molecules per cm$^2$ at the saturation coverage at 300K. The coverage dependence of the net sticking probabilities are plotted in Figure 8. Applying again the Kisluik model to the CO data an initial sticking probability of $S_0 = 0.84 \pm 0.01$ and $K = 0.28 \pm 0.01$ have been found. Both values agree very well with those reported in literature for 300 K, with K ranging from 0.26 [16] to 0.30 [5], and $S_0$ ranging from 0.80 to 0.85 [4;5;24;25].

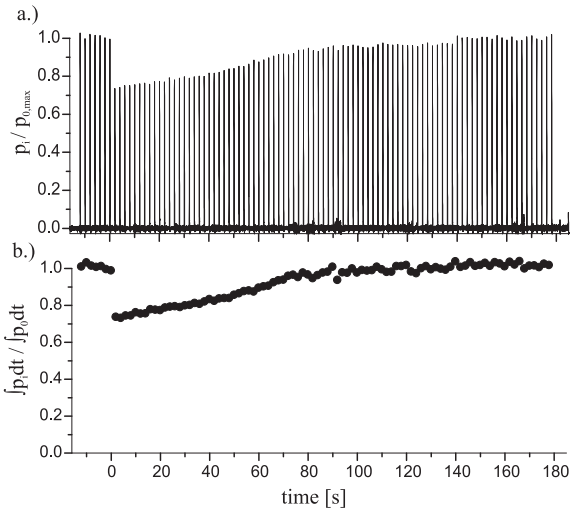


Figure 7: (a)Normalized QMS signals (28amu) for the adsorption of CO on Pt(111) at 300K. After seven pulses (each contains $4 \cdot 10^{13}$ CO molecules) the flag was opened, after 68 pulses the flag was closed again. (b)The circles refer to the normalized area under the QMS signal for each pulse.

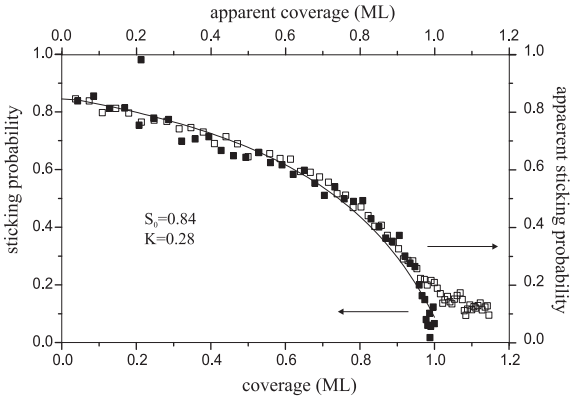


Figure 8: Coverage dependence of the net and apparent sticking probability measured for CO on clean Pt(111) at T=300K. Best fit to the net sticking probabilities using the Kisliuk eq.(4) (solid curve).

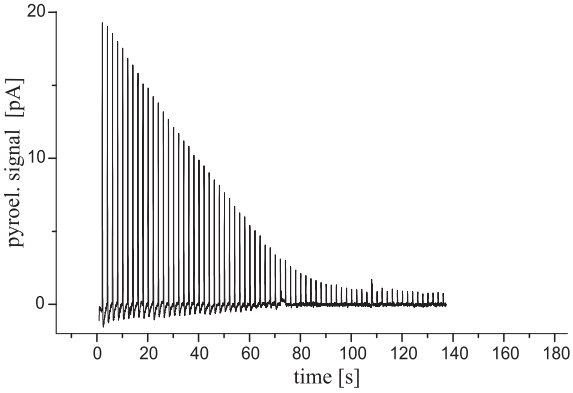


Figure 9: Pyroelectric signals for CO adsorption on Pt(111), recorded to together with the QMS data, depicted in Figure 7

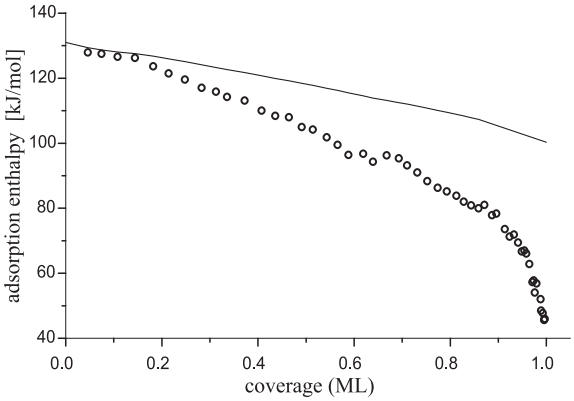


Figure 10: Coverage dependent adsorption enthalpies for CO on Pt(111) at 300 K: average of five measurements for the differential heat of adsorption (open circles), the integral heat of adsorption (thin solid line).

### *3.2.2. Microcalorimetry*

Typical pyroelectric data collected during a SCAC experiment for CO on Pt(111) are shown in Figure 9. The peak heights are decreasing in a nearly linear fashion for the first 25 CO pulses, then the pyroelectric signals decrease more slowly until a steady state is reached.

In analogy to benzene the differential molar adsorption heats $q_{cal}$ have been calculated from the heat released during each pulse and the mole number of adsorbed molecules. The differential and integrated molar adsorption enthalpies are shown in Figure 10.

The differential adsorption enthalpy declines almost linearly from initially 134kJ/mol to 80kJ/mol at ($\theta = 0.9$), followed by a rapid decrease to 45kJ/mol at the saturation coverage $\theta \approx 1$. There

Table 2: Comparison of theoretical and the experimentally measured integral heats of adsorption at $\theta = 0.5$

| $\Delta H_{ads}$ | DFT method | Ref. |
|---|---|---|
| 180kJ/mol | PW91 | Lynch et al.[17] |
| 153kJ/mol | B88+P86 | Zhang et al.[28] |
| 150kJ/mol | LDA+PW91 | Bleakley et al.[3] |
| 129kJ/mol | RPBE | Gajdos et al.[8] |
| 118kJ/mol | RPBE | Abild-Pedersen et al.[1] |
| 117kJ/mol | experimental | this work |

is a vast amount of experimental data, reporting 117kJ/mol to 146kJ/mol for the initial heat of adsorption[9],[6] **(Das sind vor allem Theorie-Zitate)**. The value found by Brown et al. from another SCAC experiment is somewhat higher (187(±11)kJ/mol)[4].

At 300K for low coverage almost all CO molecules occupy on-top sites of the Pt(111) surface. For a coverage of $\theta = 0.5$ about 80% of the CO were found on-top and only 20% is bridged-bonded[12]. In order to compare the experimentally determined adsorption heats with quantum chemical calculation done at $\theta = 0.5$, theoretically determined values for the on-top adsorption enthalpies have to be used. However, to compare the theoretical results with the experimental values one must integrate the measured differential heats of adsorption from zero up to 0.5ML. The comparison between SCAC and theory is shown in Table 2Å clear trend in the improvement of the theoretical calculations over the last few years can be seen. The older calculations were done with the Perdew-Wang-91-functional (PW91) (or the even older P86 and P88 respectively), whereas the newer investigations used the revised Perdew-Burke-Ernzerhof functionals (RPBE). The most recent quantum mechanic calculation of Abild-Pedersen and Andersson is in perfect agreement with the experimental value **(Wie gro ist denn die Wrme fr den anderen Platz?)-114kJ/mol**.

Besides the initial enthalpy of adsorption or the adsorption enthalpy at a certain coverage, the dependence of the adsorption enthalpies on coverage is also interesting. A very good agreement is found between our SCAC data and He scattering experiments of Poelsema et al.[22] and time-resolved desorption studies by Kinne et al.[12]. A linear decrease of the differential heats of adsorption is found, giving the same slope for the 3 different experiments within the error bars as seen in Table 1. This also indicates that there seems to be no additional energy barrier for desorption. However, classical TDS results from 1970s[7;20? ;21] exhibit less congruence in the slope behavior. Usually TDS spectra are evaluated using the first order kinetics Redhead equation, with a fixed value of the pre-exponential factor assumed $\upsilon = 10^{15}/s$. In contrast Seebauer et al.[24] were able to extract the coverage dependence of $\upsilon(\theta)$ from their data, starting at $10^{14.4\pm0.5}/s$ and dropping down to about $10^{7.5}/s$ at the saturation coverage. Therefore the variation of $\upsilon$ with coverage has to be considered in the evaluation of the TDS data with the Redhead equation. The importance of the coverage dependence of the pre-exponential factor is also considered in a MC simulation (McEwen).

We investigated also the desorption behavior at the saturation coverage. The apparent sticking probability and the associated apparent coverage for 300K are plotted in Figure 8. It is obvious that the net and the apparent sticking probability shows the same behavior for a coverage ranging from $\theta = 0 - 0.95$, but then the net sticking probability tends to zero, while the apparent stick probability remains finite and tends towards a constant value, i. e. at $\theta > 0.95$ a part of the CO molecules are also transiently adsorbed and become desorbed in the period of 2s between the gas pulses.

Within the kinetic model eq.(9a and 9b) also the desorption behavior of CO on Pt(111) has been analyzed. The residence time $\tau_d$ for CO molecules transiently trapped was found to be $50 \pm 20$ms at the coverage $\theta \approx 1$. Thus within the assumption that no additional activation barrier exists, $E_d + RT/2 = \Delta H_{ads} = 45kJ/mol$ we obtain a pre-exponential factor from the Arrhenius equation of $\upsilon = 2 \cdot 10^9/s$. This value points to a constrained transition state and is much smaller than the pre-exponential factors used for the evaluation of the TDS spectra. Therefore, the deviations between our SCAC data and the analysis of the TDS spectra seem to be mainly due to the coverage dependence of the pre-exponential factor.

**Zusammenfassung**

*3.3. acknowledgement*

## References


[1] Abild-Pedersen, F., Andersson, M. P., Apr. 2007. Co adsorption energies on metals with correction for high coordination adsorption sites - a density functional study. Surface Science 601 (7), 1747–1753.

[2] Ajo, H. M., Ihm, H., Moilanen, D. E., Campbell, C. T., Nov. 2004. Calorimeter for adsorption energies of larger

Table 1: Comparison of the coverage dependence of the differential adsorption enthalpies

| $\Delta H_{ads}(\theta = 0)$ | slope | range | method | Ref. |
|---|---|---|---|---|
| 134kJ/mol | $-58(\pm 2)$kJ/mol$ML$ | $0 < \theta < 0.6$ | SCAC | this work |
| 137kJ/mol | $-53(\pm 4)$kJ/mol/$ML$ | $0 < \theta < 0.7$ | LITD | Seebauer et al.[24] |
| 137kJ/mol | $-31.5(\pm 9)$kJ/mol$ML$**diff.?** | $0 < \theta < 0.8$ | time-resolved desorption | Kinne et al.[12] |
| 132kJ/mol | $-51(\pm 3)$kJ/mol$ML$ | $0 < \theta < 0.34$ | SCAC | this work |
| 133kJ/mol | $-29(\pm 10)$kJ/mol/$ML$**ehr 38?** | $0 < \theta < 0.34$ | He scattering | Poelsema et al.[22] |
| 137kJ/mol | $-8(\pm 1)$kJ/mol$ML$ | $0 < \theta < 0.9$ | TDS, Redhead $\upsilon = 10^{15}$/s | Ertl et al.[7] |


molecules on single crystal surfaces. Rev. Sci. Instr. 75 (11), 4471–4480.

[3] Bleakley, K., Hu, P., Aug. 1999. Density functional theory study of the interaction between co and on a pt surface: Co/pt(111), o/pt(111), and co/o/pt(111). Journal Of The American Chemical Society 121 (33), 7644–7652.

[4] Brown, W. A., Kose, R., King, D. A., Mar. 1998. Femtomole adsorption calorimetry on single-crystal surfaces. Chemical Reviews 98 (2), 797–831, rev.

[5] Campbell, C. T., Ertl, G., Kuipers, H., Segner, J., 1981. A molecular-beam investigation of the interactions of co with a pt(111)surface. Surface Science 107 (1), 207–219.

[6] Christoffersen, E., Stoltze, P., Norskov, J. K., May 2002. Monte carlo simulations of adsorption-induced segregation. Surface Science 505 (1-3), 200–214.

[7] Ertl, G., Neumann, M., Streit, K. M., 1977. Chemisorption of co on pt(111) surface. Surface Science 64 (2), 393–410.

[8] Gajdos, M., Eichler, A., Hafner, J., Mar. 2004. Co adsorption on close-packed transition and noble metal surfaces: trends from ab initio calculations. Journal Of Physics-Condensed Matter 16 (8), 1141–1164.

[9] German, E. D., Sheintuch, M., Sep. 2008. Comparative theoretical study of co adsorption and desorption kinetics on (111) surfaces of transition metals. Journal Of Physical Chemistry C 112 (37), 14377–14384.

[10] Ihm, H., Ajo, H. M., Gottfried, J. M., Bera, P., Campbell, C. T., Sep. 2004. Calorimetric measurement of the heat of adsorption of benzene on pt(111). Journal Of Physical Chemistry B 108 (38), 14627–14633.

[11] King, D. A., Wells, M. G., 1972. Molecular-beam investigation of adsorption kinetics on bulk metal targets - nitrogen on tungsten. Surface Science 29 (2), 454–&.

[12] Kinne, M., Fuhrmann, T., Whelan, C. M., Zhu, J. F., Pantforder, J., Probst, M., Held, G., Denecke, R., Steinruck, H. P., Dec. 2002. Kinetic parameters of co adsorbed on pt(111) studied by in situ high resolution x-ray photoelectron spectroscopy. Journal Of Chemical Physics 117 (23), 10852–10859.

[13] Kisliuk, P., 1957. The sticking probabilities of gases chemisorbed on the surfaces of solids. Journal Of Physics And Chemistry Of Solids 3 (1-2), 95–101.

[14] Kovar, M., Dvorak, L., Ĉerný, S., 1994. Application of pyroelectric properties of LiTaO3 single crystal to microcalorimetricmeasurement of the heat of adsorption. Appl. Surf. Sci. 74, 51.

[15] Kyser, D. A., Masel, R. I., Nov. 1987. Design of a calorimeter capable of measuring heats of adsorption on single-crystal surfaces. Review Of Scientific Instruments 58 (11), 2141–2144.

[16] Liu, J., Xu, M., Nordmeyer, T., Zaera, F., Apr. 1995. Sticking probabilities for co adsorption on pt(111) surfaces revisited. Journal Of Physical Chemistry 99 (16), 6167–6175.

[17] Lynch, M., Hu, P., Jun. 2000. A density functional theory study of co and atomic oxygen chemisorption on pt(111). Surface Science 458 (1-3), 1–14.

[18] Lytken, O., Lew, W., Campbell, C. T., Oct. 2008. Catalytic reaction energetics by single crystal adsorption calorimetry: hydrocarbons on pt(111). Chemical Society Reviews 37 (10), 2172–2179.

[19] Maguire, L. P., Szilagyi, S., Scholten, R. E., 2004. High performance laser shutter using a hard disk drive voice-coil actuator. Rev. Sci. Instrum. 75 (9), 3077.

[20] McCabe, R. W., Schmidt, L. D., 1977. Binding states of co on single-crystal planes of pt. Surface Science 66 (1), 101–124.

[21] NORTON, P. R., GOODALE, J. W., SELKIRK, E. B., 1979. Adsorption of co on pt(111) studied by photoemission, thermal-desorption spectroscopy and high-resolution dynamic measurements of work function. Surface Science 83 (1), 189–227.

[22] Poelsema, B., Palmer, R. L., Comsa, G., 1984. A thermal he scattering study of co adsorption on pt(111). Surf. Sci. 136 (1), 1–14.

[23] Schiesser, A., Schafer, R., Aug. 2009. Versatile piezoelectric pulsed molecular beam source for gaseous compounds and organic molecules with femtomole accuracy for uhv and surface science applications. Review Of Scientific Instruments 80 (8), 086103.

[24] Seebauer, E. G., Kong, A. C. F., Schmidt, L. D., Oct. 1986. Adsorption and desorption of no, co and h-2 on pt(111) - laser-induced thermal-desorption studies. Surface Science 176 (1-2), 134–156.

[25] Steininger, H., Lehwald, S., Ibach, H., 1982. On the adsorption of co on pt(111). Surface Science 123 (2-3), 264–282.

[26] Stuckless, J. T., Frei, N. A., Campbell, C. T., Jun. 1998. A novel single-crystal adsorption calorimeter and additions for determining metal adsorption and adhesion energies. Rev. Sci. Instr. 69 (6), 2427–2438.

[27] Stuckless, J. T., Frei, N. A., Campbell, C. T., Jan. 2000. Pyroelectric detector for single-crystal adsorption microcalorimetry: analysis of pulse shape and intensity. Sensors And Actuators B-Chemical 62 (1), 13–22.

[28] Zhang, C. J., Baxter, R. J., Hu, P., Alavi, A., Lee, M. H., Sep. 2001. A density functional theory study of carbon monoxide oxidation on the cu3pt(111) alloy surface: Comparison with the reactions on pt(111) and cu(111). Journal Of Chemical Physics 115 (11), 5272–5277.